Electron-phonon effects in graphene and armchair (10,10) single-wall carbon nanotubes

L. M. Woods and G. D. Mahan

Department of Physics and Astronomy, University of Tennessee, Knoxville, Tennessee 37996-1200
and Solid State Division, Oak Ridge National Laboratory, P.O. Box 2008, Oak Ridge, Tennessee 37831-6032

The electron-phonon interaction in low-dimensional tight-binding systems is discussed. A sheet of graphite, which is two-dimensional, and an armchair single-wall carbon nanotube (SWNT), which is quasi-one-dimensional, are taken as examples. For the modulated hopping the matrix elements for both systems are derived in the context of a two parameter model for the phonon vibrational spectrum. It is found that they (for both structures) display a deformation type of potential, and are reduced by a factor of $(1-R)$, where R depends on the phonon parameters. It is also shown that the ordinary electron-phonon coupling displays a deformation type of approximation for both systems. Next, a different type of interaction is considered—the phonon modulated electron-electron interaction. It gives two contributions—random phase approximation with one phonon line and exchange interaction with one phonon line. We find that for the two-dimensional (2D) graphene and for the quasi-1D (10,10) SWNT, the modulated hopping and exchange coupling govern the electron transport at room temperatures.

I. INTRODUCTION

Carbon nanotubes are newly discoverd nanoparticles,[1] which have unique electrical and mechanical properties. A carbon nanotube is a graphite sheet rolled into a cylinder; its diameter is much smaller than its length. Every tube is characterized by a chiral index (n,m), with n and m being two integers, which specify the carbon nanotube uniquely. Their electronic structure is either metallic or semiconducting depending on (n,m).[2] It is very important to describe the two-dimensional graphite properly and then apply the formalism to the quasi-one dimensional single-wall carbon nanotube (SWNT).

A (10,10) single-wall nanotube has a diameter of approximately 14 Å. Many calculations and experiments are focused on this kind of SWNT's.[3,4] Therefore, we take an infinitely long (10,10) tube as an example for developing further models. Some of the experiments[4–6] are dealing with ropes and bundles of SWNT's. Several groups have announced measurements on the electrical resistivity of single-wall nanotubes. They report that for single-rope samples the resistivity at $T=300$ K is in the range of 10^{-3}–$10^{-4}\Omega$ cm. The characteristic feature is that $d\rho/dT$ is positive at or near room temperatures, which indicates the metallic nature of the system.

Reference 7 indicates that the $I-V$ characteristics are linear at $T=300$ K with resistance typically of $1 M\Omega$. Reference 8 reports that at very low temperatures the conductance is quantized. This group also announced a resistance in the order of $1 M\Omega$. According to their results, the resistance at $T=300$ K appears to scale with the overlap area with the electrodes. The experiments in Ref. 9 deal with multiwall carbon nanotubes. According to this report only the outer layer contributes to the transport. The experiments indicate that even at room temperatures the conductance is quantized by one unit of $G_0=2e^2/h=77.48\ \mu$S. The nanotube behaves as a ballistic wire even at $T=300$ K. Therefore, there are two types of reported results in the literature. First, at room

temperatures the resistivity is linear with T (which is characteristic for a metallic system). Second, considering the results from Ref. 9 one could say that the SWNT is a ballistic conductor even at $T=300$ K.

To explain the mechanism of electric transport in these systems we turn towards the electron-phonon interaction, which is the deciding factor in the context of the flow of electricity and heat.

To begin the investigation of the electron-phonon coupling one needs to have proper phonon despersions. Section II is devoted to the lattice dynamics of graphene and (10,10) SWNT. A model with two parameters is proposed—the parameters are for the central force (α) and for the angle bending (β) that involves a three-body force. It turns out, that with this model, one can describe all of the features of the in-plane phonon spectrum for graphene with a suitable choice of the two parameters. The same choice for α and β is used for the armchair tube.

In Sec. III, the electron-phonon interaction for graphene is derived. The electrons are described by a tight-binding wave function. The simplest interpretation is that the vibrating ions carry the electron orbitals with them as they move—this is the so-called rigid ion approximation. In tight-binding systems, where the electrons are well localized, the rigid ion approximation is a very reasonable approach. In graphene the Fermi surface is near the K points from the Brillouin zone (BZ).[10] Only phonons with long wavelengths are involved. Instead of calculating the potential one parametrizes it by assuming that it is proportional to the relative distance between nearest neighbors. We will assume that this is true for the carbon nanotube also. The interaction Hamiltonian is written for a solid with two atoms per unit cell. It turns out that the deformation constant D of the interaction is significantly reduced by a factor that depends only on the α and β parameters from the phonon model.

Besides the traditional modulated hopping two more terms are derived for the electron-phonon interaction. One of them is the linear electron-phonon coupling, that arises from

the Coulomb interaction between the electrons and the ions. The other one is the phonon modulated electron-electron interaction and it was firstly introduced in Ref. 11. This type of interaction could be important for low-dimensional tight-binding systems. The position of the atom, which is included in the Coulomb potential is modulated by the lattice vibrations. Keeping only terms of first order in the ion displacements around equilibrium, one is able to obtain the form of the Hamiltonian.

In Sec. IV, the same derivation is given for the armchair (10,10) SWNT. The formalism developed for the modulated hopping, the linear electron-phonon coupling and the phonon modulated electron-electron interaction is applied to the nanotube by imposing discrete boundary conditions in the appropriate direction.

Section V discusses the electron self-energy for the three different types of electron-phonon coupling. For the phonon modulated electron-electron interaction two sets of Feynman diagrams are found. One of them is the random phase approximation with one phonon line. The other one is the exchange interaction with one phonon line. The contributions from both types of diagrams are discussed for the two-dimensional graphene and for the quasi-one-dimensional (10,10) nanotube.

Section VI is devoted to some numerical estimates of the electron lifetime and the electrical conductivity for the sheet of graphite and the individual (10,10) SWNT.

II. LATTICE DYNAMICS FOR GRAPHENE AND (10,10) SWNT

A. The model

A model is suggested for the phonon spectrum of a two-dimensional sheet of graphite. Since the structure and the bond lengths for an armchair (10,10) tube and graphene are very similar, one expects to obtain a very good approximation for the phonon modes of SWNT from the graphene spectrum. The measured and calculated spectrum for two-dimensional (2D) graphite can be found in Ref. 12. That report uses the Born-von Karman lattice dynamical model and interactions up to fourth neighbors are included.

The purpose of this work is not to improve on this approach, but to give a simpler alternative for the phonon dispersions. For the transport properties of an armchair SWNT one needs to incorporate the different modes and their polarizations, which is easy to do with the proposed model for the in-plain vibrations for graphene.

We assume that there are two types of forces between the atoms. One of them is a central force, which depends only on the distance between two neighboring atoms. The potential which describes this force is given by

$$V = \frac{\alpha}{2} \sum_{ij'} [(\mathbf{u}_i - \mathbf{u}_j) \cdot \hat{\mathbf{r}}_{ij}]^2, \tag{1}$$

where $\mathbf{u}_{i,j}$ are the displacements of the atoms from their equilibrium positions, $\hat{\mathbf{r}}_{i,j}$ is the unit vector between those two atoms, and α is a constant that characterizes the central force.

The second type force is due to the bond-bending between the atoms. The three-body potential was proposed in Ref. 13 for silicon. The model is described by

$$V = \frac{\beta}{2} \sum_{ijk} (\cos \theta_{ijk} - \cos \theta_0)^2, \tag{2}$$

where θ_{ijk} is the angle-formed between the $i-j$ bond and the $i-k$ bond. θ_0 is the equilibrium angle and for the hexagonal lattice is 120°. β is a characteristic constant for this type of force.

The two parameters of this model are determined by fitting them to the well-known graphene spectrum from Ref. 12.

In the graphite structure, the angle between two closest bonds is

$$\cos \theta_{ijk} = \frac{[\mathbf{r}_{ij} + (\mathbf{u}_i - \mathbf{u}_j)] \cdot [\mathbf{r}_{ik} + (\mathbf{u}_i - \mathbf{u}_k)]}{|\mathbf{r}_{ij} + (\mathbf{u}_i - \mathbf{u}_j)||\mathbf{r}_{ik} + (\mathbf{u}_i - \mathbf{u}_k)|}. \tag{3}$$

Since one is considering small displacements from equilibrium, the above expression can be expanded for small $\mathbf{u}_{i,j,k}$. After one does that, the result takes the form

$$\cos \theta_{ijk} = \left[-\frac{1}{2} - \left(\frac{\hat{\mathbf{r}}_{ij}}{2} + \hat{\mathbf{r}}_{ik} \right) \cdot (\mathbf{u}_i - \mathbf{u}_j) \right.$$

$$\left. - \left(\frac{\mathbf{r}_{ik}}{2} + \hat{\mathbf{r}}_{ij} \right) \cdot (\mathbf{u}_i - \mathbf{u}_k) \right]. \tag{4}$$

The constant $-\frac{1}{2}$ is canceled by $\cos \theta_0 = \cos 120^0 = -\frac{1}{2}$. The microscopic equations due to the combined force from the two potentials can be written. This leads to the dynamical matrix

$$\begin{bmatrix} u - X_1 & F & A & C \\ F^* & u - X_2 & C & B \\ A^* & C^* & u - X_1 & F^* \\ C^* & B^* & F & u - X_2 \end{bmatrix} \tag{5}$$

with elements

$$u = M\omega^2,$$

$$X_1 = \frac{3\alpha}{2} + \frac{45\beta}{8} + \frac{9\beta}{8} \cos Q_y a,$$

$$X_2 = \frac{3\alpha}{2} + \frac{45\beta}{8} - \frac{3\beta}{8} \cos Q_y a + \frac{3\beta}{2} \cos \frac{Q_x a \sqrt{3}}{2} \cos \frac{Q_y a}{2},$$

$$F = \frac{3\sqrt{3}\beta}{8} i \left(\sin Q_y a - 2e^{-i\frac{Q_x a\sqrt{3}}{2}} \sin \frac{Q_y a}{2} \right),$$

$$A = e^{-i(Q_x a/2\sqrt{3})} \left[\alpha e^{i(Q_x a\sqrt{3}/2)} + \left(\frac{\alpha}{2} + \frac{27\beta}{4} \right) \cos \frac{Q_y a}{2} \right],$$

$$C = -\left(\frac{\alpha\sqrt{3}}{2} - \frac{9\sqrt{3}\beta}{4} \right) ie^{-i(Q_x a/2\sqrt{3})} \sin \frac{Q_y a}{2},$$

$$B = e^{-(Q_x a/2\sqrt{3})} \left[\frac{9\beta}{2} e^{i(Q_x a\sqrt{3}/2)} + \left(\frac{3\alpha}{2} + \frac{9\beta}{4} \right) \cos\frac{Q_y a}{2} \right],$$

where $a = \sqrt{3} a_{C-C}$. The distance between two carbon atoms is $a_{C-C} = 1.42$ Å.

The goal is to solve for the normal modes for different symmetry points in the Brillouin zone of graphite since the fourth-order equation that arises from the above matrix cannot be solved analytically in general. After one obtains simplified expressions for the modes at different symmetry points, one compares with the known phonon spectrum for graphite in order to find the best numbers for the model parameters α and β.

Simple results can be found at the Γ, K, and M points in the Brillouin zone;

$$M \omega_{\Gamma,1,2}^2 = 0,$$

$$M \omega_{\Gamma,3,4}^2 = 3\alpha + \frac{27\beta}{2},$$

$$M \omega_{K,1}^2 = 3\alpha,$$

$$M \omega_{K,2}^2 = \frac{27\beta}{2},$$

$$M \omega_{K,3,4}^2 = \frac{3\alpha}{2} + \frac{27\beta}{8},$$

$$M \omega_{M,1}^2 = 3\alpha + \frac{3\beta}{2},$$

$$M \omega_{M,2}^2 = 2\alpha,$$

$$M \omega_{M,3}^2 = \alpha + \frac{27\beta}{2},$$

$$M \omega_{M,4}^2 = 6\beta.$$

Obviously, there are more constraints here than parameters. But, nevertheless, all the characteristic features of the phonon spectrum for graphene are obtained. At the Γ point the two lower modes start at zero frequency and the higher modes start from the same nonzero value. At the K point, two of the modes are degenerate—the longitudinal optical and the longitudinal acoustic modes have a common frequency.

To find the best fit for the parameters α and β one has to look at the problem of interest. Here we are interested in the longitudinal acoustic branch. A good approximation of the LA branch can be obtained by choosing $\alpha = 8.98$ N/m^2 and $\beta = 0.4$ N/m^2. The graphene spectrum for these values is presented in Fig. 1. The lower branches are described very well while the upper branches are shifted upward although they retain the general features of the graphene spectrum.

B. Phonon spectrum for a (10,10) SWNT

To obtain the phonon dispersion relations and the polarization vectors for a SWNT we explore the connection between the structure of the tube and the carbon sheet and also
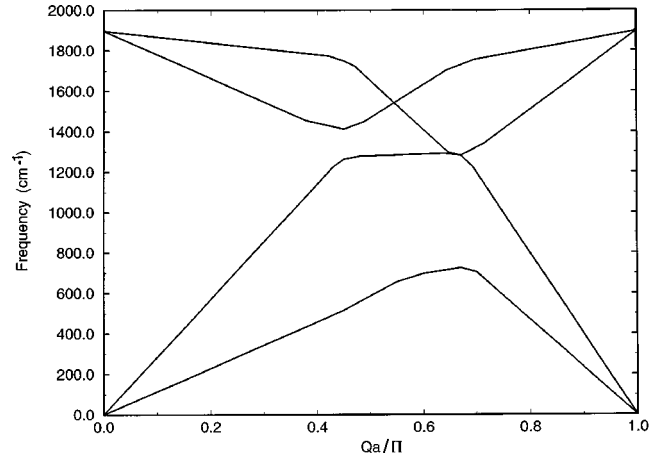

FIG. 1. Phonon spectrum for graphene with $\alpha = 8.98$ N/m^2 and $\beta = 0.4$ N/m^2.

we take into account that the tube is essentially a one-dimensional system. The translational symmetry of the armchair SWNT persists along the tube axis, but no longer around the circumference. The phonon wave vector is discrete in this direction and takes discrete values. For an armchair tube

$$Q_x = \frac{m}{N} \frac{2\pi}{\sqrt{3}a}, \tag{6}$$

where $m = 0, 1, \ldots, N$. We are interested in transport properties where the acoustic modes are important. Only the long-wave length modes and the polarization vectors around the Γ point need to be determined. Results for $m = 0$ are given on Fig. 2. α and β have the same values as for graphene.

The terms from the dynamical matrix are expanded for small wave vectors;

$$X_1 = \frac{3\alpha}{2} + \frac{27\beta}{4} - \frac{9}{16}\beta Q_y^2 a^2, \tag{7}$$

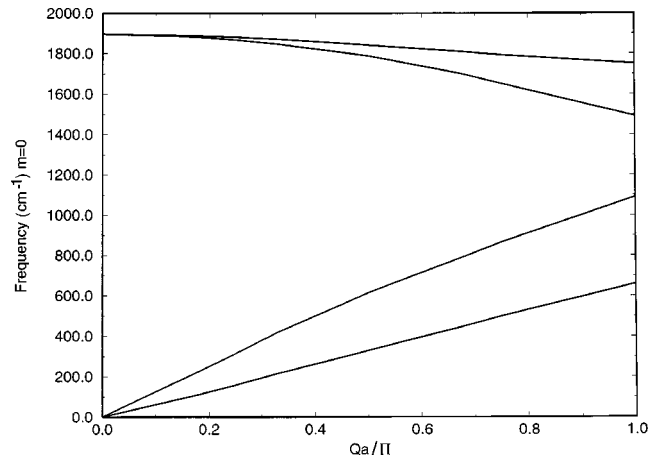$$X_2 = \frac{3\alpha}{2} + \frac{27\beta}{4} - \frac{9}{16}\beta Q_x^2 a^2, \tag{8}$$

FIG. 2. Phonon spectrum for $m = 0$ for the SWNT.

$$F = -\frac{9}{16}\beta Q_x Q_y a^2, \tag{9}$$

$$A = \frac{3\alpha}{2} + \frac{27\beta}{4} + iQ_x a \frac{\sqrt{3}}{2}\left(\frac{\alpha}{2} - \frac{9}{4}\beta\right), \tag{10}$$

$$C = -iQ_y a \frac{\sqrt{3}}{2}\left(\frac{\alpha}{2} - \frac{9}{4}\beta\right), \tag{11}$$

$$B = \frac{3\alpha}{2} + \frac{27\beta}{4} - iQ_x a \frac{\sqrt{3}}{2}\left(\frac{\alpha}{2} - \frac{9}{4}\beta\right). \tag{12}$$

Add and subtract the microscopic equations to obtain a solution for $(\eta_{A,x,y} - \eta_{B,x,y})$ in terms of $(\eta_{A,x,y} + \eta_{B,x,y})$

$$M\omega^2(\eta_{A,x} + \eta_{B,x}) = -Q_y^2 a^2 D_r(\eta_{A,x} + \eta_{B,x})$$
$$+ iQ_y a D_i(\eta_{A,x} - \eta_{B,x})$$
$$+ Q_x Q_y a^2 D_r(\eta_{A,y} + \eta_{B,y})$$
$$- iQ_y a D_i(\eta_{a,y} - \eta_{B,y}), \tag{13}$$

$$M\omega^2(\eta_{A,x} - \eta_{B,x}) = -iQ_x a D_i(\eta_{A,x} + \eta_{B,x})$$
$$+ (G - Q_y^2 a^2 D_r)(\eta_{A,x} - \eta_{B,x})$$
$$+ iQ_y a D_i(\eta_{A,y} + \eta_{B,y})$$
$$+ Q_x Q_y a^2 D_r(\eta_{A,y} - \eta_{B,y}), \tag{14}$$

$$M\omega^2(\eta_{A,y} + \eta_{B,y}) = Q_x Q_y a^2 D_r(\eta_{A,x} + \eta_{A,x})$$
$$- iQ_y a D_i(\eta_{A,x} - \eta_{B,x})$$
$$- Q_x^2 a^2 D_r(\eta_{A,y} + \eta_{B,y})$$
$$- iQ_x a D_i(\eta_{A,y} - \eta_{B,y}), \tag{15}$$

$$M\omega^2(\eta_{A,y} - \eta_{B,y}) = iQ_y a D_i(\eta_{A,x} + \eta_{B,x}) + Q_x Q_y a^2 D_r(\eta_{A,x}$$
$$- \eta_{B,x}) - iQ_x a D_i(\eta_{A,y} + \eta_{B,y})$$
$$+ (G - Q_x^2 a^2 D_r)(\eta_{A,y} - \eta_{B,y}), \tag{16}$$

$$D_r = \frac{9}{16}\beta, \tag{17}$$

$$D_i = \frac{\sqrt{3}}{4}\left(\alpha - \frac{9}{2}\beta\right), \tag{18}$$

$$G = 3\alpha + \frac{27}{2}\beta. \tag{19}$$

The subscripts A and B correspond to the two atoms in the unit cell. The acoustic modes are the ones in Eqs. (13) and (15) and the optical modes are those in Eqs. (14) and (16). They are coupled; although the acoustic modes are of interest for us, we have to include the optical modes also.

At long wavelength only the terms of first order wave vector are kept in the expressions for the optical modes. Thus, we are able to write

$$(\eta_{A,x} - \eta_{B,x}) \approx i\frac{R}{4\sqrt{3}}[Q_x a(\eta_{A,x} + \eta_{B,x})$$
$$- Q_y a(\eta_{A,y} + \eta_{B,y})], \tag{20}$$

$$(\eta_{A,y} - \eta_{B,y}) \approx -i\frac{R}{4\sqrt{3}}[Q_x a(\eta_{A,y} + \eta_{B,y})$$
$$+ Q_y a(\eta_{A,x} + \eta_{B,x})], \tag{21}$$

$$R = \frac{\alpha - 9/2\beta}{\alpha + 9/2\beta}. \tag{22}$$

If one uses our fitted values for the force constants, one can estimate that the factor $R \approx 0.67$.

The above derivations are for a two-dimensional layer of graphite. From here it is easy to derive the optical modes for a SWNT. Set $Q_x = 0$ and keep $Q_y = Q$ continuous. Then, the expressions become

$$(\eta_{A,x} - \eta_{B,x}) = -i\frac{\sqrt{3}}{12}RQa(\eta_{A,y} + \eta_{B,y}), \tag{23}$$

$$(\eta_{A,y} - \eta_{B,y}) = -i\frac{\sqrt{3}}{12}RQa(\eta_{A,x} + \eta_{B,x}). \tag{24}$$

These results are important in the determination of the matrix elements for the electron-phonon interaction as is shown in the following sections.

III. ELECTRON-PHONON INTERACTIONS IN GRAPHENE

A. Modulated hopping in terms of the tight-binding approximation

We are interested in electron-phonon coupling in graphene. The electron, that is responsible for the electric conduction, in the plane is in a p_z state. Start with the Hamiltonian

$$H = H_0 + H_{mod},$$

$$H_0 = -J_0 \sum_{j,\delta,\sigma} (c_{j,\sigma}^+ c_{j+\delta,\sigma} + c_{j+\delta,\sigma}^+ c_{j,\sigma}),$$

$$H_{mod} = -J_1 \sum_{j,\delta,\sigma} \hat{\delta} \cdot (\mathbf{u}_j - \mathbf{v}_{j+\delta})(c_{j,\sigma}^+ c_{j+\delta,\sigma} + c_{j+\delta,\sigma}^+ c_{j,\sigma}),$$

where $\hat{\delta}$ is the unit vector connecting nearest neighbors in the hexagonal structure—see Fig. 3. σ is a spin index. $J_0 = 2.6$ eV is the nearest-neighbor integral for graphite. J_1 can be taken to be $J_1 \sim q_0 J_0$, where we use $q_0 = 2.2$ Å^{-1} as in Ref. 14. Actually, J_0 is higher for the nanotube.[19] We keep the same value for both systems in order to illustrate the model better. $\mathbf{u}_j$ and $\mathbf{v}_j$ are small displacements from the equilibrium positions of the two ions in the unit cell. They are expanded in terms of the phonon creation and annihilation operators

$$\mathbf{u}_n = \sum_{\mathbf{Q}} \hat{\eta}_n e^{i\mathbf{Q}\cdot\mathbf{R}_n^0} A_{\mathbf{Q}}, \tag{25}$$
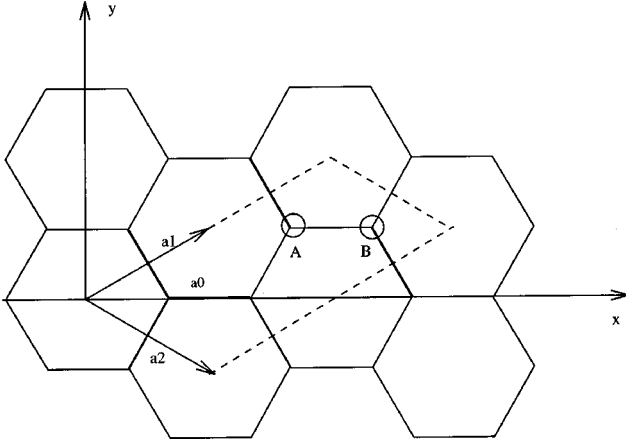
FIG. 3. Structure of a layer of graphite.

$$X_{\mathbf{Q}} = \sqrt{\frac{\hbar}{2NM\omega_{\mathbf{Q}}}}, \tag{26}$$

$$A_{\mathbf{Q}} = b^{+}_{-\mathbf{Q}} + b_{\mathbf{Q}}, \tag{27}$$

$\omega_{\mathbf{Q}}$ is the frequency of the phonons and $\hat{\boldsymbol{\eta}}_n$ is the polarization vector of the ion. Then the electron field operators are written in terms of the creation and annihilation operators for the electrons

$$\psi = \sum_{\mathbf{k}} \psi_{\lambda}(\mathbf{k}) c_{\mathbf{k},\lambda}, \tag{28}$$

where $\psi(\mathbf{k})$ is the tight-binding wave function and λ is the band index.[15] Thus, the full expression for the Hamiltonian is

$$H_{int} = \sum_{ij,nn'} \sum_{\mathbf{kk'Q}\delta} q_0 J_0 \sqrt{\frac{\hbar}{2NM\omega_{\mathbf{Q}}}} \boldsymbol{\delta} \cdot (\hat{\boldsymbol{\eta}}_n e^{i\mathbf{k} \cdot \mathbf{R}^0_n} - \hat{\boldsymbol{\eta}}_{n'} e^{i\mathbf{k} \cdot \mathbf{R}^0_{n'}})$$

$$\times [\lambda^*_i(\mathbf{k}') e^{-i(\mathbf{k}' \cdot \mathbf{R}^0_{n'} - \mathbf{k} \cdot \mathbf{R}^0_n)} + \lambda_j(\mathbf{k}) e^{-i(\mathbf{k}' \cdot \mathbf{R}^0_n - \mathbf{k} \cdot \mathbf{R}^0_{n'})}]$$

$$\times c^{+}_{\mathbf{k}',\lambda_i} c_{\mathbf{k},\lambda_j} (b_{\mathbf{Q}} + b^{+}_{-\mathbf{Q}}) \delta_{\mathbf{k}',\mathbf{k}+\mathbf{Q}}. \tag{29}$$

This is a general formula for the modulated hopping electron-phonon interaction of a solid with two atoms per unit cell. For graphene all the vectors in the above formulas are two dimensional. Now, one can evaluate the matrix elements for the electron-phonon coupling. The constants λ, which control the processes between different energy bands, are also present.

B. Deformation potential approximation

The Fermi surface[15] of the two-dimensional graphite has small circles around the K-points in the Brillouin zone. Because of the symmetry of the system it is only necessary to consider one of them, which we choose to be $\mathbf{k}_0 = (2\pi/\sqrt{3}a, 2\pi/3a)$. The excited electronic states are in the vicinity of this point and they are located in a small wave-vector space. Only the long-wave limit $\mathbf{Q} \to 0$ in the first Brillouin zone is needed and only acoustic phonons are important; take $\omega_Q = sQ$, with s being the sound velocity in the layer. Then, it is possible to write the Hamiltonian of interaction in the form

$$H_{e-ph} = D \sum_{\substack{\mathbf{kQ} \\ ij}} X_{\mathbf{Q}} |\mathbf{Q}| c^{+}_{\mathbf{k}+\mathbf{Q},\lambda_i} c_{\mathbf{k},\lambda_j'} A_{\mathbf{Q}}. \tag{30}$$

For graphene we are interested in what happens around the K point only, where the two bands cross the Fermi level. We make an expansion around these points—$\mathbf{k} \to \mathbf{k}_0 + \tilde{\mathbf{k}}$, where $\tilde{\mathbf{k}}$ is a small vector. Therefore, we expect the deformation type of approximation to be valid. One finds, that

$$E = \pm v_F |\tilde{k}|, \tag{31}$$

$$\lambda_{A,B} = \pm e^{-i\phi(k)}, \tag{32}$$

where $v_F = J_0 \sqrt{3}a/2$ and the phase factor is $\phi(k) = (2\pi/3 + \tan^{-1} \tilde{k}_x / \tilde{k}_y)$ and $i,j = A,B$. For the matrix elements in the same band (M_{11}) and between the two bands (M_{12}) we find

$$M_{\mathbf{kk'},11} = \sum_{AB} 2X_{\mathbf{Q}} q_0 J_0 e^{i(\phi' - \phi/2)}$$

$$\times \left[\hat{\boldsymbol{\eta}}_A \cdot \hat{\boldsymbol{\delta}} \cos\left(\frac{2\pi}{3} - \mathbf{k}_0 \cdot \mathbf{R}_{AB} - \frac{\mathbf{Q} \cdot \mathbf{R}_{AB}}{2} + \frac{\phi + \phi'}{2} \right) \right.$$

$$\times e^{-i(\mathbf{Q} \cdot \mathbf{R}_{AB}/2)} - \hat{\boldsymbol{\eta}}_B \cdot \hat{\boldsymbol{\delta}} \cos\left(\frac{2\pi}{3} + \mathbf{k}_0 \cdot \mathbf{R}_{BA} \right.$$

$$\left. + \frac{\mathbf{Q} \cdot \mathbf{R}_{BA}}{2} + \frac{\phi + \phi'}{2} \right) e^{-i(\mathbf{Q} \cdot \mathbf{R}_{BA}/2)} \right], \tag{33}$$

$$M_{\mathbf{kk'},22} = -M_{\mathbf{kk'},11}, \tag{34}$$

$$M_{\mathbf{kk'},12} = \sum_{AB} 2X_{\mathbf{Q}} q_0 J_0 e^{i(\phi' - \phi/2)}$$

$$\times \left[\hat{\boldsymbol{\eta}}_A \cdot \hat{\boldsymbol{\delta}} \sin\left(\frac{2\pi}{3} - \mathbf{k}_0 \cdot \mathbf{R}_{AB} - \frac{\mathbf{Q} \cdot \mathbf{R}_{AB}}{2} + \frac{\phi + \phi'}{2} \right) \right.$$

$$\times e^{-i(\mathbf{Q} \cdot \mathbf{R}_{AB}/2)} - \hat{\boldsymbol{\eta}}_B \cdot \hat{\boldsymbol{\delta}} \sin\left(\frac{2\pi}{3} + \mathbf{k}_0 \cdot \mathbf{R}_{BA} \right.$$

$$\left. + \frac{\mathbf{Q} \cdot \mathbf{R}_{BA}}{2} + \frac{\phi + \phi'}{2} \right) e^{-i(\mathbf{Q} \cdot \mathbf{R}_{BA}/2)} \right], \tag{35}$$

$$M_{\mathbf{kk'},21} = -M_{\mathbf{kk'},12}, \tag{36}$$

where $\mathbf{R}_{AB} = \mathbf{R}^0_A - \mathbf{R}^0_B$. Further manipulations are possible—take the limit for small $\mathbf{Q}$ and expand around the K point. Using the results about the calculated phonon spectrum for graphene in the previous section, one obtains

$$M_{11} = -iq_0 J_0 X_{\mathbf{Q}} \frac{\sqrt{3}}{4} \bigg[(\eta_{Ax} + \eta_{Bx})$$

$$\times \bigg(Q_x a \cos\frac{\phi + \phi'}{2} + Q_y a \sin\frac{\phi + \phi'}{2} \bigg) + (\eta_{Ay} + \eta_{By})$$

$$\times \bigg(Q_x a \sin\frac{\phi + \phi'}{2} - Q_y a \cos\frac{\phi + \phi'}{2} \bigg) \bigg] (1 - R), \quad (37)$$

$$M_{12} = -iq_0 J_0 X_{\mathbf{Q}} \frac{\sqrt{3}}{4} \bigg[(\eta_{Ax} + \eta_{Bx})$$

$$\times \bigg(Q_x a \sin\frac{\phi + \phi'}{2} - Q_y a \cos\frac{\phi + \phi'}{2} \bigg) + (\eta_{Ay} + \eta_{By})$$

$$\times \bigg(Q_x a \cos\frac{\phi + \phi'}{2} + Q_y a \sin\frac{\phi + \phi'}{2} \bigg) \bigg] (1 - R). \quad (38)$$

The following conclusions can be made. First, the matrix elements for both transitions—intraband and interband—are in the deformation type form and they are reduced by a factor $(1-R)$, which depends on the parameters chosen to describe the oscillations of the ions. Our choice for α and β gives that $R \approx 0.67$. Second, it is evident that not only the longitudinal modes are important, but also the transverse modes give a similar contribution. Both types of polarizations are present in M_{11} and M_{12}. The formulas (37) and (38) disagree with the ones found in Ref. 14 by a factor $(1-R) \sim 0.33$. Also the dependance of $|M_Q|^2$ on the phonon wave vector Q is clearly displayed in the present calculation.

C. Electron-phonon and phonon-modulated electron-electron interactions

The model is a neutral tight-binding systems that has two atoms per unit cell. For graphite the ion cores have s-wave symmetry and the electrons that are responsible for the conduction process p_z-wave symmetry. Since this is a neutral system the average number of conduction carriers on each side is equal to the valence of the ions. We also assume that the rigid ion approximation is valid and the electrons can hop to the neighboring sites. The problem can be approached in a more general way starting from the Hamiltonian

$$H = H_0 + H_{int}, \quad (39)$$

$$H_0 = -J_0 \sum_{j\delta} (A_{j+\delta}^+ B_j + B_{j+\delta}^+ A_j) + \sum_{\mathbf{Q}} \omega_{\mathbf{Q}} a_{\mathbf{Q}}^+ a_{\mathbf{Q}}, \quad (40)$$

$$H_{int} = \frac{e^2}{2} \sum_{nn'} \int \frac{d^3 r_1 d^3 r_2}{|\mathbf{r}_1 - \mathbf{r}_2|} [\rho_i(\mathbf{r}_1 - \mathbf{R}_n) - \rho_e(\mathbf{r}_1 - \mathbf{R}_n) c_n^+ c_n]$$

$$\times [\rho_i(\mathbf{r}_2 - \mathbf{R}_{n'}) - \rho_e(\mathbf{r}_2 - \mathbf{R}_{n'}) c_{n'}^+ c_{n'}], \quad (41)$$

where ρ_i and ρ_e are the ion and electron charge densities. By A_j and B_j we denote the electron operators for the two ions in the unit cell. The formalism for a crystal with one atom per unit cell was already developed in Ref. 11. Here, we perform the same calculation for a solid with two atoms per unit cell. We want to express H_{int} in terms of collective coordinates. The first thing that needs to be done is to diagonalize H_0. This could be done by using Eq. (40) and applying the transformation

$$A_{\mathbf{k}} = \frac{1}{\sqrt{2}} (\alpha_{\mathbf{k}} + \beta_{\mathbf{k}}), \quad (42)$$

$$\tilde{B}_{\mathbf{k}} = \frac{1}{\sqrt{2}} (\alpha_{\mathbf{k}} - \beta_{\mathbf{k}}), \quad (43)$$

with $\tilde{B}_{\mathbf{k}} = e^{i\theta(\mathbf{k})} B_{\mathbf{k}}$, where $\theta(\mathbf{k})$ is the phase factor of $e^{i\delta\cdot\mathbf{k}}$. Only nearest neighbors are taken into consideration. For small k around the K point in the BZ $\theta(\mathbf{k})$ coincides with $\phi(k)$ defined earlier in Eq. (32). The next step is to take the Fourier transformation of the Coulomb potential and of the charge densities. According to Ref. 16 the wave function for the ions is given by $\psi_{2s} = |c_i| r e^{-\alpha_i r/2}$. The normalization condition gives that $|c_i|^2 = \alpha_i^5/96\pi$. Therefore, one can easily find

$$\rho_i(q) = \int d^3 r \rho_i(r) e^{i\mathbf{q}\cdot\mathbf{r}} = Z\alpha_i^6 \frac{\alpha_i^2 - q^2}{(\alpha_i^2 + q^2)^4}, \quad (44)$$

where Z is the number of electrons in the ion.

For the conduction electrons in graphite we take that $\psi_{2p_z} = |c_e| \mathbf{r}\cdot\hat{\mathbf{n}} e^{-\alpha_e r/2}$—the free electrons are in $2p_z$ atomic orbitals.[16] To proceed further adopt a coordinate system with z axis along the q vector;

$$\hat{\mathbf{q}} \cdot \hat{\mathbf{r}} = \cos\theta,$$

$$\hat{\mathbf{q}} \cdot \hat{\mathbf{n}} = \cos\theta_0,$$

$$\hat{\mathbf{r}} \cdot \hat{\mathbf{n}} = \cos\theta \cos\theta_0 + \sin\theta \sin\theta_0 \cos\phi.$$

Thus, the expression for $\rho_e(q)$ is found to be

$$\rho_e(q) = \frac{16\pi |c_e|^2 \alpha_e}{(q^2 + \alpha_e^2)^4} [(3\cos^2\theta_0 - 1)(\alpha_e^2 - 5q^2)$$

$$+ 3\sin^2\theta_0 (\alpha_e^2 - q^2)]. \quad (45)$$

θ_0 is the angle between $\mathbf{q}$ and the normal vector to the graphene plane $\hat{\mathbf{n}}$. The normalization of the used $2p_z$-wave functions determines the constant $|c_e|^2$. One finds $|c_e|^2 = \alpha_e^5/(32\pi)$ and the expression for the electron density turns out to be

$$\rho_e(q) = \frac{\alpha_e^6}{(\alpha_e^2 + q^2)^3}. \quad (46)$$

Note that the angle between $\mathbf{q}$ and the normal vector to the graphite plane is $\theta_0 = 90°$.

It is possible to obtain several terms from the Hamiltonian from Eq. (41). One of them is the traditional modulated hopping for which we find the same results for the matrix elements as in Eqs. (37) and (38) providing the expressions are expanded for small k around the K point. Another term is the electron-phonon interaction, which is written as

$$H_{e-p} = \frac{i}{\Omega} \sum_{\mathbf{Q}} X_{\mathbf{Q}} v_{\mathbf{Q}} \rho_T(\mathbf{Q}) \rho_e(\mathbf{Q})$$

$$\times \mathbf{Q} \cdot [(\hat{\eta}_A e^{i[\theta(\mathbf{k}-\mathbf{Q})-\theta(\mathbf{k})]} + \widehat{\eta_B})(\alpha^+_{\mathbf{k}+\mathbf{Q}}\alpha_{\mathbf{k}} + \beta^+_{\mathbf{k}+\mathbf{Q}}\beta_{\mathbf{k}})$$

$$- (\hat{\eta}_A e^{i[\theta(\mathbf{k}-\mathbf{Q})-\theta(\mathbf{k})]} - \hat{\eta}_B)(\alpha^+_{\mathbf{k}+\mathbf{Q}}\beta_{\mathbf{k}}$$

$$+ \beta^+_{\mathbf{k}+\mathbf{Q}}\alpha_{\mathbf{k}})]A_{\mathbf{Q}}, \tag{47}$$

$$\rho_T(Q) = \rho_i(Q) - Z\rho_e(Q). \tag{48}$$

The above formulas are investigated for longitudinal phonons—$\hat{\eta}_{A,B} = \hat{\eta}_{\mathbf{Q}}$. In the limit of small wave vector $\mathbf{Q}$ we find that

$$\tilde{D} = v_{\mathbf{Q}}\rho_T(\mathbf{Q})\rho_e(\mathbf{Q}) = 4\pi Z e^2 \left[\frac{3}{\alpha_e^2} - \frac{5}{\alpha_i^2}\right]. \tag{49}$$

Therefore, the matrix elements for the electron-phonon interaction are of the form of a deformation potential with a deformation constant $\tilde{D}$. For transitions in the same band and between bands up to a phase factor we find

$$M_{11} = 2X_{\mathbf{Q}}\tilde{D}\mathbf{Q}_\perp \cos\left[\frac{\theta(\mathbf{k}-\mathbf{Q})-\theta(\mathbf{k})}{2}\right], \tag{50}$$

$$M_{12} = 2X_{\mathbf{Q}}\tilde{D}\mathbf{Q}_\perp \sin\left[\frac{\theta(\mathbf{k}-\mathbf{Q})-\theta(\mathbf{k})}{2}\right], \tag{51}$$

where $\mathbf{Q}_\perp$ is the phonon wave vector in the graphite plane.

The last term is the phonon modulated electron-electron coupling. This interaction is produced by multiplying the terms that contain ρ_e in Eq. (41). The expression is practically the same as in Ref. 11. Its origin comes from the interaction of the electrons and phonons through the Coulomb potential, which is modulated by the lattice vibrations of the solid. One finds that there are four possible combinations

$$\sum_{nn'=A,B} \rho_n(\mathbf{q}+\mathbf{Q})\rho_{n'}(-\mathbf{q})$$

$$= \rho_A(\mathbf{q}+\mathbf{Q})\rho_A(-\mathbf{q}) + \rho_A(\mathbf{q}+\mathbf{Q})\rho_B(-\mathbf{q})$$
$$+ \rho_B(\mathbf{q}+\mathbf{Q})\rho_A(-\mathbf{q}) + \rho_B(\mathbf{q}+\mathbf{Q})\rho_B(-\mathbf{q}), \tag{52}$$

$$\rho_A(\mathbf{q}) = A^+_{\mathbf{k}+\mathbf{q}}A_{\mathbf{k}}, \tag{53}$$

$$\rho_B(\mathbf{q}) = e^{i[\theta(\mathbf{k}-\mathbf{q})-\theta(\mathbf{k})]}\tilde{B}^+_{\mathbf{k}+\mathbf{q}}\tilde{B}_{\mathbf{k}}. \tag{54}$$

In general, processes are possible between any combination of four bands. To determine the matrix elements correctly one needs to put all phase factors that depend on the physical structure of the solid. The complete expression for H_{e-ph-m} for the different transitions is given below;

$$H_{e-ph-m} = -\frac{4i}{\Omega} \sum_{\mathbf{kk'qQ}} e^{-(\theta_1+\theta_2)/2} X_{\mathbf{Q}}(\mathbf{q} \cdot \hat{\eta}_{\mathbf{Q}}) v_{\mathbf{q}}\rho_e^2(\mathbf{q})A_{\mathbf{Q}}$$

$$\times \left[(\alpha^+_{\mathbf{k}+\mathbf{q}+\mathbf{Q}}\alpha^+_{\mathbf{k'}-\mathbf{q}}\alpha_{\mathbf{k}}\alpha_{\mathbf{k'}} + \alpha^+_{\mathbf{k}+\mathbf{q}+\mathbf{Q}}\beta^+_{\mathbf{k'}-\mathbf{q}}\alpha_{\mathbf{k}}\beta_{\mathbf{k'}} + \beta^+_{\mathbf{k}+\mathbf{q}+\mathbf{Q}}\beta^+_{\mathbf{k'}-\mathbf{q}}\beta_{\mathbf{k}}\beta_{\mathbf{k'}} + \beta^+_{\mathbf{k}+\mathbf{q}+\mathbf{Q}}\alpha^+_{\mathbf{k'}-\mathbf{q}}\beta_{\mathbf{k}}\alpha_{\mathbf{k'}})\cos\frac{\theta_1}{2}\cos\frac{\theta_2}{2} \right.$$

$$- (\alpha^+_{\mathbf{k}+\mathbf{q}+\mathbf{Q}}\alpha^+_{\mathbf{k'}-\mathbf{q}}\alpha_{\mathbf{k}}\beta_{\mathbf{k'}} + \alpha^+_{\mathbf{k}+\mathbf{q}+\mathbf{Q}}\beta^+_{\mathbf{k'}-\mathbf{q}}\alpha_{\mathbf{k}}\alpha_{\mathbf{k'}} + \beta^+_{\mathbf{k}+\mathbf{q}+\mathbf{Q}}\beta^+_{\mathbf{k'}-\mathbf{q}}\beta_{\mathbf{k}}\alpha_{\mathbf{k'}} + \beta^+_{\mathbf{k}+\mathbf{q}+\mathbf{Q}}\alpha^+_{\mathbf{k'}-\mathbf{q}}\beta_{\mathbf{k}}\beta_{\mathbf{k'}})i\cos\frac{\theta_1}{2}\sin\frac{\theta_2}{2}$$

$$- (\alpha^+_{\mathbf{k}+\mathbf{q}+\mathbf{Q}}\alpha^+_{\mathbf{k'}-\mathbf{q}}\beta_{\mathbf{k}}\alpha_{\mathbf{k'}} + \beta^+_{\mathbf{k}+\mathbf{q}+\mathbf{Q}}\alpha^+_{\mathbf{k'}-\mathbf{q}}\alpha_{\mathbf{k}}\alpha_{\mathbf{k'}} + \beta^+_{\mathbf{k}+\mathbf{q}+\mathbf{Q}}\beta^+_{\mathbf{k'}-\mathbf{q}}\alpha_{\mathbf{k}}\beta_{\mathbf{k'}} + \alpha^+_{\mathbf{k}+\mathbf{q}+\mathbf{Q}}\beta^+_{\mathbf{k'}-\mathbf{q}}\beta_{\mathbf{k}}\beta_{\mathbf{k'}})i\sin\frac{\theta_1}{2}\cos\frac{\theta_2}{2}$$

$$\left. - (\alpha^+_{\mathbf{k}+\mathbf{q}+\mathbf{Q}}\alpha^+_{\mathbf{k'}-\mathbf{q}}\beta_{\mathbf{k}}\beta_{\mathbf{k'}} + \alpha^+_{\mathbf{k}+\mathbf{q}+\mathbf{Q}}\beta^+_{\mathbf{k'}-\mathbf{q}}\beta_{\mathbf{k}}\alpha_{\mathbf{k'}} + \beta^+_{\mathbf{k}+\mathbf{q}+\mathbf{Q}}\alpha^+_{\mathbf{k'}-\mathbf{q}}\alpha_{\mathbf{k}}\beta_{\mathbf{k'}} + \beta^+_{\mathbf{k}+\mathbf{q}+\mathbf{Q}}\beta^+_{\mathbf{k'}-\mathbf{q}}\alpha_{\mathbf{k}}\alpha_{\mathbf{k'}})\sin\frac{\theta_1}{2}\sin\frac{\theta_2}{2} \right], \tag{55}$$

where

$$\theta_1 = \theta(\mathbf{k}+\mathbf{q}+\mathbf{Q}) - \theta(\mathbf{k}),$$

$$\theta_2 = \theta(\mathbf{k'}-\mathbf{q}) - \theta(\mathbf{k'}).$$

The matrix elements in general could be written as a part that is common to all processes and a part that depends on the phase factors. The term that appears in all transitions we denote as

$$|M_{q,Q}| = 4M_q(\mathbf{q} \cdot \hat{\eta}_{\mathbf{Q}})X_{\mathbf{Q}}, \tag{56}$$

$$M_q = v_q\rho_e^2(q). \tag{57}$$

Having the expressions for the matrix elements one is able to proceed with further calculations.

IV. ELECTRON-PHONON INTERACTIONS IN A (10,10) SWNT

A. Deformation potential approximation for the modulated hopping

The length of a SWNT is much larger than its diameter. Observed lengths of (10,10) armchair tubes are of several

μm and the diameter of an individual tube is approximately 14 Å. It is essentially a quasi-one dimensional system.[4,17]

The whole formalism of describing the carbon nanoparticles was already developed in the previous section, where we discussed a two dimensional sheet of graphite. For the nanotube, the Fermi surface is collapsed into two symmetric points K and K' at $\pm 2\pi/3a$, where a is the length of the primitive translational vector[18]—see Fig. 3.

In the circumferential directions only discrete wave vectors are allowed. The appropriate boundary conditions for an armchair tube are

$$k_x = \frac{m}{N}\frac{2\pi}{\sqrt{3}a}, \tag{58}$$

where $m = 0, 2, \ldots, N-1$. The $k_y = k$ wave vector, which is along the tube axis, is kept continuous. The energy dispersion relations can be obtained in this way.[19] The lowest bands in all armchair tubes are nondegenerate and they cross the Fermi level. Thus, an armchair tube is expected to be a metal—only infinitesimal excitations are needed to excite carriers into the conduction band.[19]

Again we are interested in carrier excitations around the K points in the Brillouin zone. Thus, for the expansion $k = k_0 + \tilde{k}$, where $k_0 = 2\pi/3a$ and $\tilde{k}$ is small, one finds

$$E = \pm v_F \tilde{k}, \tag{59}$$

$$\lambda_{A,B} = \pm e^{-i(2\pi/3)}, \tag{60}$$

where $v_F = J_0\sqrt{3}a/2$. As in graphene one obtains a linear k dependence in the energy with the difference that k is a one dimensional vector ($\tilde{k}$ is renamed back to k).

The evaluation of the matrix elements is based on the matrix elements for graphene, given in Eqs. (33)–(36). The summations over nearest neighbors are done and the expressions simplify to

$$M_{kk+Q,11} = 2q_0 J_0 X_Q$$
$$\times \left\{ (\eta_{Ax} - \eta_{Bx})\left[1 + \cos\frac{Qa}{4}\cos\left(\frac{\pi}{3} + \frac{Qa}{4}\right)\right] \right.$$
$$\left. + \sqrt{3}i(\eta_{Ay} + \eta_{By})\sin\frac{Qa}{4}\cos\left(\frac{\pi}{3} + \frac{Qa}{4}\right) \right\}, \tag{61}$$

$$M_{kk+Q,12} = 2q_0 J_0 X_Q\left[i(\eta_{Ax} + \eta_{Bx})\sin\frac{Qa}{4}\sin\left(\frac{\pi}{3} + \frac{Qa}{4}\right) \right.$$
$$\left. + \sqrt{3}(\eta_{Ay} - \eta_{By})\cos\frac{Qa}{4}\sin\left(\frac{\pi}{3} + \frac{Qa}{4}\right) \right]. \tag{62}$$

Further insight can be gained by using the deformation potential approximation. Taking the limit of a small wave vector k around the K point and a small phonon vector Q the matrix elements become

$$M_{11} = 2q_0 J_0 X_Q\left[\frac{3}{2}(\eta_{Ax} - \eta_{Bx}) + (\eta_{Ay} + \eta_{By})i\frac{\sqrt{3}}{8}Qa\right], \tag{63}$$

$$M_{12} = 2q_0 J_0 X_Q\left[(\eta_{Ax} + \eta_{Bx})i\frac{\sqrt{3}}{8}Qa + \frac{3}{2}(\eta_{Ay} - \eta_{By})\right]. \tag{64}$$

Next, use Eqs. (23) and (24) to eliminate $(\eta_{A,xy} - \eta_{B,xy})$. The final form for the matrix elements for the modulated hopping is

$$M_{11} = q_0 J_0 X_Q\frac{\sqrt{3}}{4}Qa(\eta_{Ay} + \eta_{By})(1-R), \tag{65}$$

$$M_{12} = q_0 J_0 X_Q\frac{\sqrt{3}}{4}Qa(\eta_{Ax} + \eta_{Bx})(1-R). \tag{66}$$

The matrix elements are reduced by $(1-R)$, which depends on the parameters α and β—the constants which characterize the phonon spectrum for the tube. Since $(1-R) \sim 0.33$ then squaring the matrix element causes a significant reduction of $(1-R)^2 \sim 0.1$. The same result was found for graphene. Again the modulated hopping is written in terms of the deformation potential approximation.

Compare with the results from Ref. 20. Both calculations give similar results about the dependance on the phonon wave vector Q. The major difference is that the matrix elements here are shown to be reduced by a factor $(1-R)$, because of the coupling between the acoustic and optical phonons.

B. Electron-phonon and phonon-modulated electron-electron interactions

All the formulas developed previously for the two dimensional graphite layer are expected to be valid here. The expressions for the electron charge density and ion charge density are the same as for graphene.

Consider the electron-phonon interaction. The Hamiltonian has the same form as in Eq. (47). The deformation constant $\tilde{D}$ is also the one derived for graphene. The only difference here is that the electron and phonon wave vectors are one dimensional. The phase factor $\theta(\mathbf{k})$ is also involved in the expression for the matrix elements. For a (10,10) SWNT it was already derived that it is a constant $\theta(\mathbf{k}) = -2\pi/3$. Therefore,

$$M_{11} = -iX_{Q_z}\tilde{D}Q_z, \tag{67}$$

$$M_{12} \sim Q_z^2. \tag{68}$$

Transitions between two different bands to first order of the phonon wave vector are not allowed in the armchair tube. The fact that $M_{12} \sim Q^2$ is a consequence of the coupling between acoustic and optical phonons and of the one dimensionality of the system.

Consider the new contribution to the electron-phonon interaction which is the phonon modulated electron-electron interaction. We obtain the matrix elements from Eq. (55). For the tube $\theta_1 = 0$ and $\theta_2 = 0$ because the phase factors are constants. Therefore, only the first term survives and the matrix element up to a phase factor is given by the expression

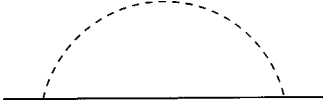$$M_{q_z,Q_z} = -4iM_{q_z}(\mathbf{q}\cdot\hat{\eta}_\mathbf{Q})X_{Q_z}. \tag{69}$$

FIG. 4. Feynman diagram for first-order electron-phonon interaction.

FIG. 5. Feynman diagram for the RPA with one phonon line.

Different matrix elements are obtained corresponding to different electron-phonon coupling processes. The expressions for the different terms in the original Hamiltonian—Eq. (41)—is rather general and it can be applied to other tight-binding systems. The idea is that the effects of several contributions with different origin are comparable for low-dimensional systems and the evaluation of the transport characteristics needs to be done carefully.

For small wave vectors $q_z \ll \alpha$ the bare Coulomb potential is a good approximation.

Notice that the above was done assuming that this is essentially a one-dimensional system. But carbon nanotubes have finite diameters and are quasi-one dimensional. The Coulomb interaction for electrons on a cylinder with radius R is modified to[21]

$$M_{qQ} = \alpha' I_L(qR) K_L(qR) \sqrt{\frac{\hbar}{2NM\omega_Q}} i(\mathbf{q} \cdot \hat{\xi}_Q). \quad (70)$$

$I_L(qR)$ and $K_L(qR)$ are the modified Bessel functions from first and second kind of the order L—which stands for angular momentum of the interaction. If $L=0$ then we are dealing with a intraband transitions; if $L=1$ then the transitions are interband. But in this case transitions between bands do not take place and therefore L is always zero.

V. ELECTRON SELF-ENERGY

A. Modulated hopping and linear electron-phonon interaction

The imaginary part of the electron self-energy is a very important quantity. It is closely related to the relaxation time of the electrons

$$-\mathrm{Im}\Sigma(\mathbf{k}) = \frac{\hbar}{2\tau}. \quad (71)$$

Several transport properties depend on the self-energy. Here we will examine the impact of different types of interactions on it.

The first effect is how the imaginary part of the self-energy depends on the electron-phonon interaction. The basic diagram is given on Fig. 4. It has one phonon line represented by a dashed line. This diagram represents two types of the electron-phonon interaction—the modulated hopping and the linear electron-phonon coupling.

The expression for the self energy is well-known and in the high temperature limit is given by[22]

$$-\mathrm{Im}\Sigma(\mathbf{k}) = 2\pi(k_B T) \sum_{\mathbf{Q}} \frac{|M_{\mathbf{Q}}|^2}{\hbar\omega_{\mathbf{Q}}} \delta(\epsilon_{\mathbf{k}} - \epsilon_{\mathbf{k}+\mathbf{Q}}). \quad (72)$$

Thus, we obtain that $-\mathrm{Im}\Sigma(\mathbf{k})$ is proportional to the temperature T, which is characteristic for a metallic system. The matrix elements are already derived and they are of deformation type with different deformation constants. This
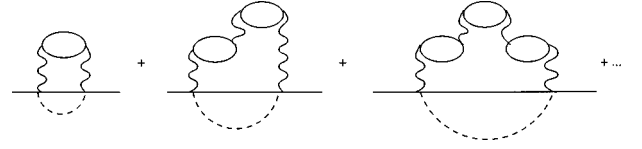
means that one needs to do the above integration once and then use the appropriate deformation constant.

Consider the quasi-one-dimensional armchair SWNT. Using the known energy dispersion—$\epsilon_k = \pm v_F |k - k_F|$ we find

$$\frac{\hbar}{2\tau} = (k_B T) \frac{|C|^2 L_0}{2M} \int_{-\pi/a}^{\pi/a} dQ \frac{Q^2}{\omega_Q^2} \delta(\epsilon_k^i - \epsilon_{k+Q}^j), \quad (73)$$

$$\frac{1}{\tau} = \frac{(k_B T)}{\hbar} \frac{|C|^2 L_0}{2Ms^2 v_F}, \quad (74)$$

where we used $\omega_Q = sQ$, with s being the speed of sound in the graphite plane. The band indices are $i,j = 1,2$ and L_0 is the length of the unit cell in 1D. C is the deformation constant and it is either D or $\tilde{D}$ for the modulated hopping or the linear electron-phonon coupling. A nonzero answer is obtained only for the case $i \neq j$, so only intraband transitions give contributions to the self energy.

For graphene we perform the same integration. The δ function is used to do the integration over the angular variable. The result is

$$\frac{1}{\tau} = \frac{(k_B T)}{\hbar} \frac{|C|^2 A_0}{4\pi Ms^2 v_F^2} \epsilon_k, \quad (75)$$

where A_0 is the area of the unit cell and ϵ_k is the energy of the electron.

B. RPA with one phonon line for the phonon modulated Coulomb interaction

Besides the contribution to the electron self energy from the modulated hopping and ordinary electron-phonon interaction, there is a contribution from the phonon modulated electron-electron interaction. It was already shown, that there are two sets of Feynman diagrams that correspond to it. One of them is the random phase approximation with one phonon line—see Fig. 5. Using Lehmann representation it was derived that in 2D and 3D, in general, the contribution to the self-energy from the RPA could be neglected.[11]

Some analytical results for the RPA diagrams can be obtained for SWNT due to the one dimensionality of the system. The self energy for the RPA diagrams, after the summation over iQ_n is done, is

$$\Sigma(k) = \frac{\hbar}{2NM\beta} \sum_{iq_n} \sum_{q,Q} \frac{(\hat{\eta}_Q \cdot \mathbf{Q})^2}{\omega_Q} \frac{M_q^2 P_q}{\epsilon_{RPA}}$$

$$\times \left[\frac{N_Q + f''}{iq_n + ik_n + \omega_Q - \epsilon''} + \frac{1 + N_Q - f''}{iq_n + ik_n - \omega_Q - \epsilon''} \right], \quad (76)$$

where the following definitions are made

$$P_q = 2 \int \frac{dk}{(2\pi)} \frac{f_k - f_{k+q}}{iq_n + \epsilon_k - \epsilon_{k+q}},$$

$$\epsilon_{RPA} = 1 - M_q P_q,$$

$$N_Q = 1/(e^{\beta\omega_Q} - 1),$$

$$f'' = 1/(e^{\beta\epsilon_{k+q+Q}} + 1).$$

M_q is the electron-electron interaction for the nanotube and it is taken to be the Coulomb interaction in 1D. P_q is the polarization factor for the bubble. It is only for excitations in the same band. This is obtained by considering the correlation function for the Green's function, which needs to be evaluated in order to construct the Feynman diagrams. This means that the two lines making the bubble belong to the same band. Using the fact that $f(-x) = 1 - f(x)$ for the Fermi distribution function one is able to arrive at

$$P_q = 2 \int \frac{dk}{2\pi} (f_k - f_{k+q}) \frac{2(\epsilon_k - \epsilon_{k-q})}{(\epsilon_k - \epsilon_{k-q})^2 - (iq_n)^2}, \quad (77)$$

where

$$\epsilon_k - \epsilon_{k-q} = v_F q. \quad (78)$$

In the limit for small q one finds

$$P_q = \frac{v_F q^2}{\pi[(v_F q)^2 - (iq_n)^2]}. \quad (79)$$

The polarization factor has poles at $\pm v_F q$. The dielectric function becomes

$$\epsilon_{RPA} = 1 + \frac{v_F M_q q^2/\pi}{(iq_n)^2 - (v_F q)^2}. \quad (80)$$

To obtain the correct result for the electron self energy all of the frequency summations have to be done before making the continuation $ik_n \to \epsilon_k + i\delta$. The summation over iq_n can be easily performed in Eq. (76)

$$\Sigma(\mathbf{k}) = \frac{\hbar v_F}{NM\pi} \sum_{qQ} \frac{(\hat{\eta}_Q \cdot \mathbf{Q})^2}{\omega_Q} \frac{q^2 M_q^2}{M_q'} \cdot \left\{ \left[\frac{N(M_q') + f(\epsilon'' - \omega_Q)}{ik_n + M_q' + \omega_Q - \epsilon''} \right. \right.$$

$$\left. + \frac{1 + N(M_q') - f(\epsilon'' - \omega_Q)}{ik_n - M_q' + \omega_Q - \epsilon''} \right] (N_Q + f'')$$

$$+ \left[\frac{N(M_q') + f(\epsilon'' + \omega_Q)}{ik_n + M_q' - \omega_Q - \epsilon''} + \frac{1 + N(M_q') - f(\epsilon'' + \omega_Q)}{ik_n - M_q' - \omega_Q - \epsilon''} \right]$$

$$\left. \times (1 + N_Q - f'') \right\}, \quad (81)$$

where

$$M_q'^2 = (v_F q)^2 \left(1 - \frac{M_q}{v_F} \right), \quad (82)$$

$$N(M_q') = 1/(e^{\beta M_q'} - 1), \quad (83)$$

$$f(\epsilon'' \pm \omega) = 1/(e^{\beta(\epsilon'' \pm \omega)} + 1), \quad (84)$$

$$\epsilon'' = \epsilon_{k+q+Q}. \quad (85)$$

Now, the imaginary part of the electron self energy can be found by substituting $ik_n \to \epsilon_k + \delta$. One notes that two terms can be found in the high-temperature limit. One is proportional to T^2 and the other one is linear with T.

The term proportional to T^2 is

$$\frac{\hbar}{2\tau} = \frac{2(k_B T)^2 v_F L_0}{NM} \sum_{qQ,ij} \frac{(\hat{\eta}_Q \cdot \mathbf{Q})^2}{\omega_Q^2} \frac{q^2 M_q^2}{M_q'^2}$$

$$\times [\delta(\epsilon_{i,k} - \epsilon_j'' - M_q') + \delta(\epsilon_{k,i} - \epsilon_j'' + M_q')]. \quad (86)$$

Making use of the δ function we obtain

$$\frac{1}{\tau} = \frac{16(k_B T)^2 L_0 e^4 k_F}{\pi^2 \hbar v_F^2 M s^2} \times I, \quad (87)$$

$$I = \int_0^1 \frac{\ln^2 x}{1 - \frac{2e^2}{v_F} \ln x}, \quad (88)$$

where $I = 0.17$. There are two terms proportional to T;

$$-\text{Im}\Sigma(k)_1 = \frac{v_F(k_B T)}{2NM} \sum_{qQ} \frac{(\eta_Q \cdot \mathbf{Q})^2}{\omega_Q^2} \frac{q^2 M_q^2}{M_q'} \delta(\epsilon_{i,k} - \epsilon_j'') \quad (89)$$

$$-\text{Im}\Sigma(k)_2 = \frac{\hbar v_F(k_B T)}{2NM} \sum_{qQ} \frac{(\hat{\eta} \cdot \mathbf{Q})^2}{\omega_Q} \frac{q^2 M_q^2}{M_q'^2} \delta(\epsilon_{i,k} - \epsilon_j''). \quad (90)$$

From here one can estimate that only $-\text{Im}\Sigma_2$ survives and for the lifetime we find

$$\frac{1}{\tau} = |k - k_F| \frac{8(k_B T)e^4 L_0 k_F}{\pi^2 M s v_F^2} \times I. \quad (91)$$

It follows that $1/\tau \sim v_F |k - k_F|$. The above formula is obtained only for transitions between the two bands. The intraband transitions give zero result.

C. Exchange self-energy

One can look beyond the RPA approximation by assuming that the effects from the exchange phonon modulated electron-electron interaction are not small.[11] It comes from the different ways of pairing of the electron operators. There are four diagrams that correspond to the exchange interaction—see Fig. 6. In the problem for graphene the pairing has to be done for two different operators present in the expression—$\alpha_\mathbf{k}$ and $\beta_\mathbf{k}$. The exchange interaction up to a phase factor is written as
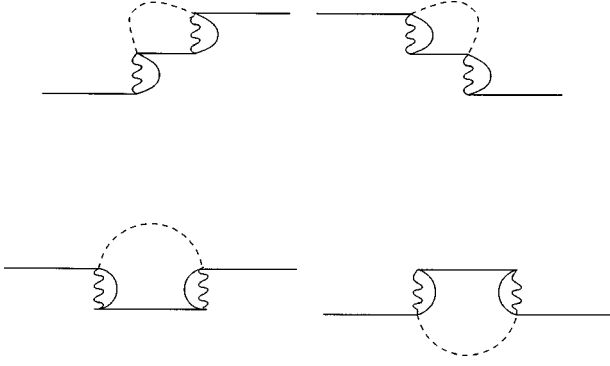
FIG. 6. Feynman diagrams for the exchange interaction with one phonon line.

$$V_{exch} = -\sum_{\mathbf{k},\mathbf{q},\mathbf{Q}} X_{\mathbf{Q}}(\mathbf{q}\cdot\mathbf{Q}) v_{\mathbf{q}}\rho_e^2(\mathbf{q})\left[f(\epsilon_{\mathbf{k}+\mathbf{q}+\mathbf{Q}}+f(\epsilon_{\mathbf{k}-\mathbf{q}})\right]$$

$$\times\left[\cos\frac{\theta(\mathbf{k}+\mathbf{Q})-\theta(\mathbf{k})}{2}(\alpha_{\mathbf{k}+\mathbf{Q}}^+\alpha_{\mathbf{k}}+\beta_{\mathbf{k}+\mathbf{Q}}^+\beta_{\mathbf{k}})\right.$$

$$\left.+\sin\frac{\theta(\mathbf{k}+\mathbf{Q})-\theta(\mathbf{k})}{2}(\alpha_{\mathbf{k}+\mathbf{Q}}^+\beta_{\mathbf{k}}+\beta_{\mathbf{k}+\mathbf{Q}}^+\alpha_{\mathbf{k}})\right]. \quad (92)$$

The Hamiltonian can be expressed in the following way

$$V_{exch} = -\sum_{\mathbf{Q},nn'} U(\mathbf{k},\mathbf{Q}) X_{\mathbf{Q}} c_{\mathbf{k}+\mathbf{Q},n}^+ c_{\mathbf{k},n'} A_{\mathbf{Q}}, \quad (93)$$

where we define

$$U(\mathbf{k},\mathbf{Q})_{ii} = \hat{\eta}_{\mathbf{Q}}\cdot[(\mathbf{k}+\mathbf{Q})S(\mathbf{k}+\mathbf{Q})$$

$$-\mathbf{k}S(\mathbf{k})]\cos\frac{\theta(\mathbf{k}+\mathbf{Q})-\theta(\mathbf{k})}{2}, \quad (94)$$

$$U(\mathbf{k},\mathbf{Q})_{ie} = \hat{\eta}_{\mathbf{Q}}\cdot[(\mathbf{k}+\mathbf{Q})S(\mathbf{k}+\mathbf{Q})-\mathbf{k}S(\mathbf{k})]$$

$$\times\sin\frac{\theta(\mathbf{k}+\mathbf{Q})-\theta(\mathbf{k})}{2}, \quad (95)$$

$$S(\mathbf{k}) = \frac{1}{k^2}\sum_{\mathbf{q}} M_q f_{\mathbf{k}-\mathbf{q}}\mathbf{k}\cdot\mathbf{q}. \quad (96)$$

For small wave vectors $\mathbf{Q}$ one is able to write

$$U(\mathbf{k},\mathbf{Q}) \approx (\hat{\eta}_{\mathbf{Q}}\cdot\mathbf{Q})S(\mathbf{k}). \quad (97)$$

Now, the one-phonon self-energy is obtained

$$\Sigma(\mathbf{k}) = \frac{\hbar S^2(\mathbf{k})}{2\rho}\sum_{\mathbf{Q}}\frac{(\hat{\eta}_Q\cdot\mathbf{Q})^2}{\omega_Q}\left[\frac{N_Q+f(\epsilon')}{ik_n-\epsilon'+\omega_Q}\right.$$

$$\left.+\frac{1+N_Q-f(\epsilon')}{ik_n-\epsilon'-\omega_Q}\right], \quad (98)$$

$$f(\epsilon') = 1/(e^{\beta\epsilon'}+1), \quad (99)$$

$$\epsilon' = \epsilon_{\mathbf{k}+\mathbf{Q}}. \quad (100)$$

In the high-temperature limit, neglecting the phonon energy compared to the electron energy,

$$-\text{Im}\Sigma(\mathbf{k}) = 2(k_B T)S^2(\mathbf{k})\sum_{\mathbf{Q}}\frac{(\hat{\eta}_{\mathbf{Q}}\cdot\mathbf{Q})^2}{\rho\omega_{\mathbf{Q}}^2}\delta(\epsilon_{\mathbf{k}}-\epsilon_{\mathbf{k}+\mathbf{Q}}). \quad (101)$$

The result looks the same as the one derived for the modulated hopping and the linear electron-phonon coupling— Eq. (72). This is not a surprise since the exchange interaction was written in a form of a deformation type of interaction.

The next step is to evaluate the function $S(\mathbf{k})$, which is contained in $U(\mathbf{k},\mathbf{Q})$. It serves the role of a deformation constant for the exchange interaction. In a more general way $S(x)$ could be written as

$$S_{1D,2D}(x) = -\frac{e^2 k_F}{2\pi}J_{1D,2D}(x). \quad (102)$$

In the Appendix we derive $J(x)$ in 1D and 2D. From there it is estimated that $J_{1D}(x=1)=0.77$ and $J_{2D}(x=1)=1.17$.

There is a direct analogy between these three types of electron-phonon interaction. Thus, to estimate τ one needs to use Eqs. (74) and (75) and substitute S_{1D} and S_{2D} instead of C.

VI. CONDUCTIVITY

First, we consider the electrical conductivity of the two-dimensional graphite. It can be estimated by the formula

$$\sigma_{gr} = e^2\langle v_x\rangle^2 N(\epsilon_F)\tau_{gr}, \quad (103)$$

where $N(\epsilon_F)$ is the number of states. Following Ref. 15. $N(\epsilon_F) = 4A_0\epsilon/3\pi J_0^2 a^2$. For graphene with a circular Fermi surface $\langle v_x\rangle^2 = \frac{1}{2}v^2$, with v being the velocity of the electron. We use the value given for the carbon nanotube—$v = 8.1\times10^5$ m/s.[8] We obtained that the lifetime of the charge carriers is $\tau\sim\epsilon_k^{-1}$ for all processes. Following Mathiessen's rule

$$\frac{1}{\tau} = \frac{1}{\tau_1}+\frac{1}{\tau_2}+\cdots. \quad (104)$$

The conductivity is a quantity that does not depend on the energy of the particles. One readily obtains that

$$\sigma_{gr} = \frac{4e^2\langle v_x\rangle^2 M s^2\hbar}{(|D|^2+|S_{2D}|^2+|\tilde{D}|^2)(k_B T)}. \quad (105)$$

Only the modulated hopping and the exchange scattering will contribute to the electron transport. Their dominance is guaranteed by the fact that the deformation constants for these two processes are an order larger than the deformation constant for the linear electron-phonon interaction. Using the expressions for the constants one finds $|D|=3.87$ eV, $|\tilde{D}|=0.87$ eV, and $|S_{2D}|=4.46$ eV. Thus, the contribution from the electron-phonon deformation constant is neglected.

One estimates that $\sigma_{gr} = 7.87 \times 10^{-2}$ S. Compare to the accepted value $\sigma_{gr} \sim 4 \times 10^{-2}$ S. The contribution from the RPA with one phonon line is not significant.

The situation with the carbon nanotube is the following. The standard formula for the conductivity in 1D is

$$\sigma_{tube} = \frac{2e^2 v \tau}{\pi \hbar}, \tag{106}$$

where τ is the relaxation time determined from all processes, that contribute to the transport. The resultant τ is found from the Mathiessen's rule according to Eq. (104). The factor of 2 indicates that there are two bands that cross the Fermi level. The dominant processes are the modulated hopping and the exchange interactions. The relaxation time due to these processes is a constant. The numerical value is obtained to be $\tau = 7.57 \times 10^{-14}$ s. The linear electron-phonon coupling is neglected as having a small deformation constant. The RPA contribution should also be neglected, because $|k - k_F|$ is small compared to the constant terms.

Another term to the lifetime is proportional to T^{-2}, which is a signature of a relaxation time due to the traditional electron-electron interaction. We estimate that $\tau = 4.18 \times 10^{-8}$ s at room temperature. A typical electron-electron relaxation time in a metallic system is of the order of 10^{-10} s. This kind of process has a much slower time than the one for the processes involving phonons at room temperatures, thus, it is neglected.

Therefore, one finds that the electrical transport properties are governed by a constant lifetime, determined from two processes—modulated hopping and exchange ineteraction. The estimated value for the resistance of the single wall nanotube is $3.16 \times 10^5 \Omega$, which agrees with the measured values by Refs. 5, 6, and 8.

As it was mentioned earlier, one group[9] has announced that an individual metallic SWNT will exhibit ballistic transport not only at low temperatures, but also at $T = 300$ K. For the ballistic transport to occur the following condition must be true—$L \ll L_m, L_\phi$, where L is the length of the sample, $L_m = v\tau$ is the mean free path and L_ϕ is phase coherence length. $v = 8.1 \times 10^5$ m/s is the velocity of the electrons. The length of the tube typically is $L = 1 - 10$ μm. We derived that the electron lifetime is finite and it corresponds to $L_m \approx 61$ nm. This shows that the mean free path is smaller than the size of the sample and the nanotube at room temperature is not in the ballistic regime.

VII. CONCLUSIONS

Several important results were obtained by the above calculations. First, we were able to derive the matrix elements of three types of the electron-phonon coupling—modulated hopping, linear electron-phonon coupling, and phonon modulated electron-electron interaction, which all displayed a deformation type of approximation. The matrix elements for the modulated hopping for graphene and SWNT are reduced due to the fact that the acoustic modes are coupled to the optical ones. This was found by introducing a two parameter model for the description of the phonon spectra for the two systems.

Up to now only the contribution from the modulated hopping was considered for these tight-binding systems.[14,20] Now due to the reduction one expects that other processes could be important. To see which type of interaction is dominant compare the deformation constants—$|D| = 3.87$, $|\overline{D}| = 0.87$, $S_{1D} = 3.03$, and $S_{2D} = 4.56$ eV. Therefore, the modulated hopping and the exchange interaction give similar contributions in agreement with Ref. 11 and the ordinary electron-phonon interaction could be neglected.

Second, it was found that for graphene $1/\tau \sim \epsilon_k$ with ϵ_k being the energy of the electron. The interesting fact is that the relaxation time is energy dependent $\tau \sim \epsilon_k^{-1}$, but the electrical conductivity is constant. The modulated hopping and the exchange scatterings give similar contributions and the RPA with one phonon line can be neglected. The accepted value for σ_{gr} is approximately 4×10^{-2} Ω^{-1}, which is in a good agreement with our numerical estimates.

Third, we obtained that in the quasi-one-dimensional metallic SWNT the important contribution comes from the same processes as in graphene—modulated hopping and exchange interaction. We find that the lifetime of the charge carriers is constant, which leads to a constant mean free path. The numerical value for τ corresponds to L_m smaller than the size of the sample. Thus, the electron transport is governed by the electron-phonon interaction at room temperatures and the nanotube is not in the ballistic regime. This is in disagreement with the experimental results, presented by Ref. 9. The conclusion from our theoretical derivations is that the nanotube should behave as a 1D metallic system at $T = 300$ K. The estimated value for the resistance is in a good agreement with the resistance given by Refs. 5, 6, and 8.

APPENDIX

The function $S(\mathbf{k})$ in 1D and 2D is evaluated here. Using the definition in 1D we have

$$S(k)_{1D} = \frac{1}{2\pi k} \int dq M_q f_{k-q} q. \tag{A1}$$

Now the change of variables $k - q \to k$ is made and the integration is restricted in the first Brillouin zone. Thus,

$$M_q = 2e^2 \ln \frac{q}{k_F} \tag{A2}$$

$$S(k)_{1D} = -\frac{e^2 k_F}{2\pi x}[(1+x)^2 \ln|1+x| - (1-x)^2 \ln|1-x| - 2x] \tag{A3}$$

$$S(k) = -\frac{e^2 k_F}{2\pi} J_{1D}(x) \tag{A4}$$

where $x = k/k_F$. Since we are interested at processes around the Fermi level we take $x = 1$ and the above expressions become

$$S(1) = -\frac{e^2 k_F}{2\pi} J_{1D}(1) \tag{A5}$$

$$J_{1D}(1) = 4 \ln 2 - 2. \tag{A6}$$

Therefore, $J_{1D}(x) \approx 0.77$.

The analytical evaluation of $S(\mathbf{k})$ in 2D is more difficult because the integration now becomes two-dimensional. After the appropriate change of variables $\mathbf{k} - \mathbf{q} \rightarrow \mathbf{k}$ we obtain

$$S(k)_{2D} = -\frac{e^2}{2\pi k} \int_0^{k_F} dk' \int_0^{2\pi} d\phi \frac{kk' - k'^2 \cos\phi}{\sqrt{k'^2 + k^2 - 2kk' \cos\phi}}. \tag{A7}$$

If the integration over ϕ is done first, this leads to elliptical integrals. It turns out that simple results can be obtained if we integrate over k' first. With $x = k/k_F$ the above expression becomes

$$S_{2D}(x) = -\frac{e^2 k_F}{2\pi x} \int_0^{2\pi} \left[\left(\frac{3}{2} x \cos\phi - x^2 \right) + \left(x - \frac{1 + 3x \cos\phi}{2} \right) \right.$$
$$\times \sqrt{1 + x^2 - 2x \cos\phi} + x^2 \left(\cos\phi - \frac{3\cos^2\phi - 1}{2} \right)$$
$$\left. \times \ln \frac{\sqrt{1 + x^2 - 2x \cos\phi} + 1 - x \cos\phi}{x(1 - \cos\phi)} \right]. \tag{A8}$$

Now at $x = 1$ the $S(x)$ function can be written in the usual form —

$$S(x) = -\frac{e^2 k_F}{2\pi} J_{2D}(x). \tag{A9}$$

$J_{2D}(x)$ is evaluated when $x = 1$

$$J_{2D}(x = 1) = \int_0^{2\pi} d\phi \left[\left(\frac{3}{2} \cos\phi - 1 \right) + (1 - 3\cos\phi) \sin\frac{\phi}{2} \right.$$
$$\left. + \frac{1}{2} (2\cos\phi - 3\cos^2\phi + 1) \ln \left(1 + \frac{1}{\sin\frac{\phi}{2}} \right) \right]. \tag{A10}$$

The above integral can be done and we obtain that $J_{2D}(x = 1) \approx 1.17$.

[1] S. Iijima and T. Ichihashi, Nature (London) **363**, 603 (1993).

[2] J.W. Mintmire, B.I. Dunlap, and C.T. White, Phys. Rev. Lett. **68**, 631 (1992).

[3] Y.-K. Kwon, S. Saito, and D. Tomanek, Phys. Rev. B **58**, R13 314 (1998).

[4] A. Thess *et al.*, Science **273**, 483 (1996).

[5] M. Bockrath *et al.*, Science **275**, 1922 (1997).

[6] J.E. Fisher *et al.*, Phys. Rev. B **55**, R4921 (1997).

[7] A. Bezryadin *et al.*, Phys. Rev. Lett. **80**, 4036 (1998).

[8] Sander J. Tans *et al.*, Nature (London) **386**, 474 (1997).

[9] Stefan Frank *et al.*, Science **280**, 1744 (1998).

[10] S. Barisic, J. Labbe, and J. Friedel, Phys. Rev. Lett. **25**, 919 (1970).

[11] G.D. Mahan and L.M. Woods, Phys. Rev. B **60**, 5276 (1999).

[12] R.A. Jishi, L. Venkataraman, M.S. Dresselhaus, and G. Dresselhaus, Chem. Phys. Lett. **209**, 77 (1993).

[13] F.H. Stillinger and T.A. Weber, Phys. Rev. B **31**, 5262 (1985).

[14] L. Pietronero, S. Strassler, and H.Z. Zeller, Phys. Rev. B **22**, 904 (1980).

[15] P.R. Wallace, Phys. Rev. **71**, 622 (1947).

[16] E. Clementi and C. Roetti, At. Data Nucl. Data Tables **14**, 282 (1974).

[17] S. Iijima, Nature (London) **354**, 56 (1991).

[18] R. Saito *et al.*, Phys. Rev. B **46**, 1804 (1992).

[19] M.S. Dresselhaus, G. Dresselhaus, and P.C. Eklund, *Science of Fullerenes and Carbon Nanotubes* (Academic Press, San Diego, 1996).

[20] R.A. Jishi, M.S. Dresselhaus, and G. Dresselhaus, Phys. Rev. B **48**, 11 385 (1993).

[21] M.F. Lin and K.W.-K. Shung, Phys. Rev. B **47**, 6617 (1993).

[22] G.D. Mahan, *Many-Particle Physics* (Plenum Press, New York, 1990).